

## Dispersion Behavior of Solutes in an Ideal Laminar Flow with Small-Bore Glass Tubes<sup>†</sup>

Takashi KORENAGA,\* Fenghua SHEN, Hirofumi YOSHIDA, and Teruo TAKAHASHI

Department of Applied Chemistry, Faculty of Engineering, Okayama University,  
Tsushima, Okayama 700

(Received September 14, 1988)

The dispersion behavior of solute molecules injected as a sample plug into an ideal laminar capillary flow was experimentally analyzed by means of microscopic and microphotometric methods. The flow pattern in small-bore glass tubes was directly observed by the microscopic method using a camera. The peak responses obtained for the colored solutes by means of the microphotometric method consist of double-humped peak features which resulted from both laminar flow convection and the molecular diffusion of solute molecules at the parabolic interface between the sample plug and the carrier fluid. The influences of the diffusion coefficient of the solute, the flow rate, the tube length, the tube diameter, etc. were mainly investigated in order to guide the design and optimization of the flow systems of capillary liquid chromatography (CLC), capillary electrophoresis (CEP), flow-injection analysis (FIA), etc. The experimental results obtained here are in good agreement with the theoretical results obtained by the numerical solution for the diffusion-convection equation.

Many open-tubular glass capillary columns have been utilized in the fields of analytical separation chemistry, such as in gas or liquid chromatography, since 1956.<sup>1)</sup> Their main advantage is in the use of long glass capillary columns in order to obtain a high resolution, but it is difficult to operate and provide instrumentation for the apparatus. Therefore, an understanding of the dispersion behavior of the solute molecules in the sample plug flowing with the carrier stream through a small-bore glass tube or the characterization of the response peak feature is important in designing flow systems with or for capillary liquid chromatography (CLC), capillary electrophoresis (CEP), flow-injection analysis (FIA), electrokinetic chromatography (EKC), field-flow fractionation (FFF), membrane-separation analysis (MSA), etc. In CLC, for example, the band broadening is just an important parameter to obtain a higher sensitivity and resolution, and it is mainly controlled by the eddy diffusion from unions, joints, and connectors,<sup>2)</sup> the molecular diffusion in both mobile and stationary phases, and the interactions between stationary and mobile phases.<sup>3)</sup>

For the dispersion phenomena in straight open tubes, several theoretical approaches have been studied in order to overcome the above-mentioned problems,<sup>4–8)</sup> but few experimental studies have been carried out. Recently, though, Atwood and Golay<sup>9)</sup> theoretically and experimentally reported the dispersion behavior of peak features using short, straight tubes in LC systems. In their experiments, however, a usual chromatographic apparatus was used, and it was difficult to obtain an ideal laminar flow because of the turbulence resulting from the sample injection, unions, joints, connectors, or the detector flow cell. Since the theoretical analyses were based on the

assumption that the capillary flow was completely laminar, a model apparatus which achieves an ideal laminar flow should be used for the experimental research.

The present authors<sup>10)</sup> previously analyzed the transport phenomena and dispersion behavior of a small quantity of a sample solution injected as a plug into a carrier fluid flowing through open-tubular small-bore tubes and built a simple simulation without considering the molecular diffusivities of the solutes in the sample-solution plug.

The present paper will mainly describe some experimental results on sample-dispersion behavior obtained for open tubular and small-bore glass capillary tubes with a circular cross-section using some diffusive solutes or a nondiffusive one in the injected sample plug. Using an ideally-composed model experimental apparatus with the microcomputer developed here, we investigated the fundamental dispersion behavior and transport phenomena of the solute dissolved in the sample solution plug in order to compare them quantitatively with the theoretical results obtained by the numerical solution for Taylor's diffusion-convection equation.<sup>4)</sup>

### Experimental

**Apparatus.** A schematic description of the experimental apparatus used for taking photographs continuously is given in Fig. 1. It is simply constructed of a Furue (Tokyo, Japan) model JP-V-W microfeeder-type syringe pump, an Olympus (Tokyo, Japan) model BH-2 microscope (equipped with an Olympus model OM-2N camera with a motor-drive unit and a shutter control unit), and various kinds (various diameters and lengths) of small-bore (capillary: less than 1 mm i.d.) glass tubes.

In order to investigate the dispersion behavior, the residence-time distribution of solutes injected as a plug were measured by means of a hand-made microphotometric detection system, as is shown in Fig. 2. The detector is mainly constructed of a Sugiura (Tokyo, Japan) model SL-

<sup>†</sup> This paper was partly presented at the 7th International Symposium on Capillary Chromatography, held in May, 1986, at Gifu, Japan.

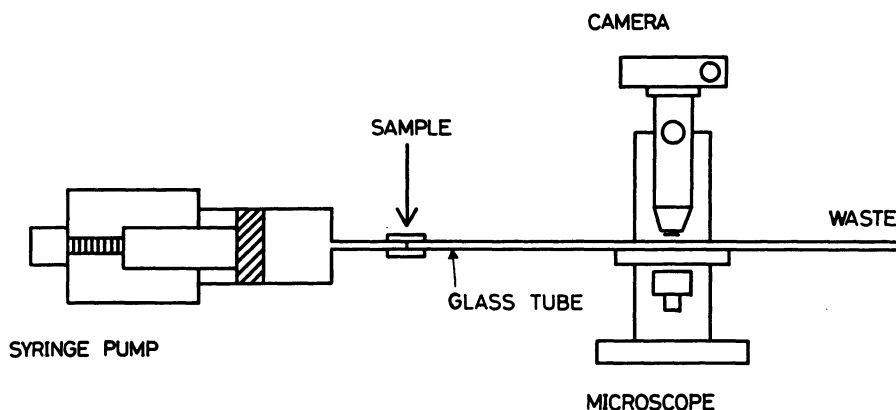


Fig. 1. Experimental apparatus with a microscope as a detector.

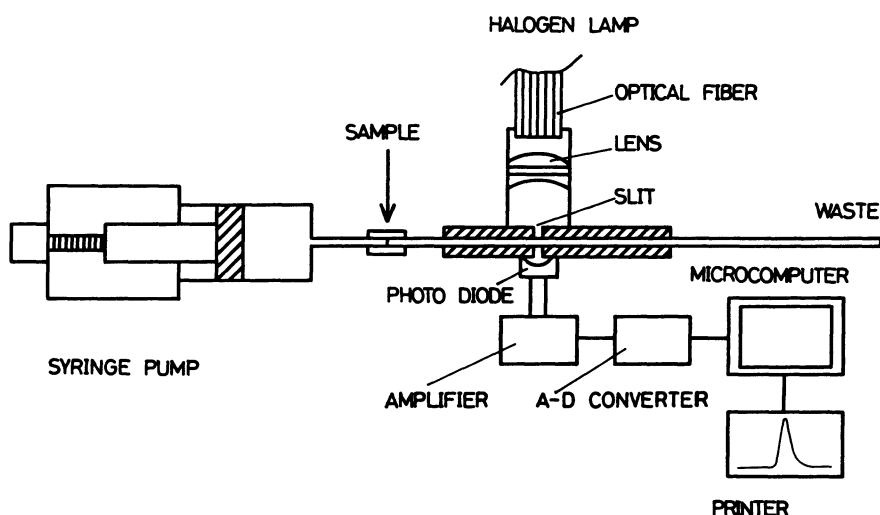


Fig. 2. Model experimental apparatus with a hand-made microphotometric detection system.

FI-150T cold light source using a halogen lamp and an optical fiber, a Hamamatsu Photonics model S-1033-01 photodiode, an Analog Devices model 757N logarithmic amplifier, and a data-recording and -processing system using a Sharp model MZ-80C microcomputer.

**Reagents.** Colored aqueous sample solutions of potassium permanganate, Methylene Blue dye (MB; Colour Index 52015), and commercially available blue ink containing submicron pigment particles were used in the present experiments. The potassium permanganate solution was prepared by dissolving analytical-reagent-grade potassium permanganate in distilled water. The dye solution was directly prepared by dissolving analytical-reagent-grade MB dye (Wako Pure Chemicals, Japan) in distilled water. The ink solution was prepared from a commercial submicron pigment ink (Sakura Color Products, Japan) by removing relatively large particles using a centrifugal separation technique. The molecular diffusion coefficient of potassium permanganate in water at a concentration of  $2.5 \times 10^{-3} \text{ mol l}^{-1}$  is  $1.2 \times 10^{-3} \text{ mm}^2 \text{ s}^{-1}$ ,<sup>4</sup> and that of MB in water is  $3.0 \times 10^{-4} \text{ mm}^2 \text{ s}^{-1}$ .<sup>10</sup> The ink consists of colored submicron pigment particles, and its molecular diffusion coefficient is

assumed to be about  $10^{-5} \text{ mm}^2 \text{ s}^{-1}$ , so that the dispersion in water occurs mainly by means of the laminar-flow convection. Distilled water and glycerol/water (1+1) mixture were used as the carrier fluids in this work.

**Procedure.** A small portion of the sample solution, dissolved in the respective carrier fluid, was injected precisely by the use of a micro syringe into a stopped-flow carrier fluid, and the syringe pump was then immediately started. By this open-column sample-injection method, the dead volumes, abrupt changes in the internal diameter, and disturbances of the flow can be reduced to a minimum. The injected sample volume was less than  $10 \mu\text{l}$ , and the injected sample length was less than 12 mm in the 1.0 mm-i.d. glass capillary column.

In the photographic experiments, a motor-drive camera was started as soon as the sample zone entered in the view of the microscope. Many photographs were taken at every 0.25 s. In the case of microphotometric detection, the BASIC program for data recording was started when the pump started. The signals obtained from the photodiode were transmitted to the microcomputer after the conversion of the analog signals to digital ones. The data stored on floppy

disk were then treated and printed out to a dotted printer or a X-Y plotter to observe the response-peak features.

## Results

**Theory on Laminar-Flow Model of Sample Plug in Small-Bore Tube.** In small-bore capillary tubes, the flow pattern of the nondiffusive sample plug can theoretically be described as a laminar-flow profile. The diameters of the capillary tubes used in this research are below 1 mm, and the average flow rates are below  $110 \text{ mm s}^{-1}$ , so the Reynolds number is smaller than 110, much smaller than the critical Reynolds number of the laminar flow (2000–2300) in a round pipe.

The velocity profile of the laminar flow may be described as follows:

$$u_r = 2u(1 - r^2/R^2) \quad (1)$$

where  $u_r$  denotes the flow rate at the tube radius  $r$  of the capillary and where  $u$  and  $R$  denote the average flow rate and the tube radius respectively. Equation 1 shows that the laminar-flow velocity profile has a parabolic dispersion of the injected sample plug and that the velocity profile possesses a large possibility of the molecular diffusion of the solute molecules caused by the concentration gradient. Equation 1 shows that the smaller the tube radius, the steeper the parabolic profile (velocity gradient) in capillary columns.

Assuming that the solute molecule used in a sample solution is nondiffusive, the following equation is obtained:

$$d_s = 2ut \quad (2)$$

where  $d_s$  and  $t$  denote the traveling distance of the sample zone head (front) and time respectively.

The apparent sample arrival time at the detection point  $t_a$ , that is, the time required for the sample-zone front to reach the detector, can be calculated for the nondiffusive solute molecules by means of Eq. 3:

$$t_a = d_s/(2u) \quad (3)$$

where the  $d_s$  nearly equals the tube length of the capillary column ( $L$ ), since short joint tubes are necessary in column connections.

For diffusive solute molecules, the baseline-to-baseline time  $\Delta t_b$ , which is the band-width in time, was investigated as a means of measuring the dispersion behavior in the response-peak profile. Vanderslice et al.<sup>8)</sup> solved Taylor's convection-diffusion equation by the finite differential method and obtained Eq. 4 for the calculation of  $\Delta t_b$ :

$$\Delta \tau_b = 1.93X^{0.64} \quad (4)$$

where  $\Delta \tau_b$  and  $X$  denote the dimensionless baseline-to-baseline time and the dimensionless traveling distance respectively, as defined by Eqs. 5 and 6:

$$\Delta \tau_b = D\Delta t_b/R^2 \quad (5)$$

$$X = DL/(2R^2u) \quad (6)$$

where  $D$  denotes the molecular diffusion coefficient of the solute in the injected sample plug.

**Evaluation of the Apparatus by Eye Measurement of Sample-Dispersion Behavior.** The traveling distances ( $d_{MB}$ ) of the colored-sample-zone front as a function

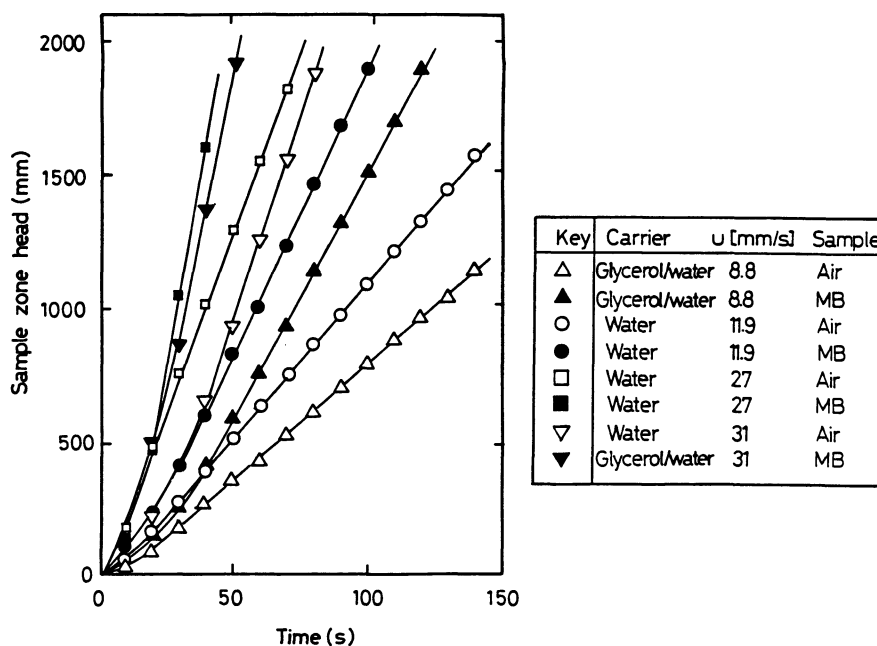


Fig. 3. Relationship between traveling distance of sample zone head and time.

of the time were measured with the eye for the solute molecules of MB dye (Fig. 3). The traveling distances of the air-segment front ( $d_{\text{air}}$ ), which was injected instead of the colored-sample-solution plugs containing solute molecules, were also represented as typical examples for the comparison of the dispersion behavior. When the air segment is injected, the flow rate of the air segment just equals the average flow rate ( $u$ ) of the carrier fluid according to Eq. 2. In the case of the plots for the air segment, the slopes of the curves equal  $u$  except for each transition period. The laminar capillary-flow model of the MB solute in the injected sample plug is shown in Fig. 4(a). The traveling distances of the front interface of the MB solute were smaller than that calculated by Eq. 2. This might be because the MB molecule diffuses to the radial direction at the interface of the sample plug. The component substance (i.e., the MB solute) at the front interface of the sample plug naturally diffuses to the low-velocity-gradient region in the laminar capillary

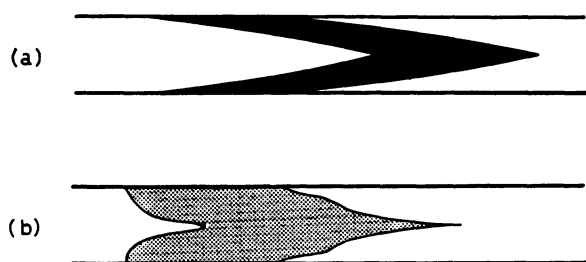


Fig. 4. Models of the flowing sample plug zones in laminar capillary flow. (a) Nondiffusive solute, (b) diffusive solute.

flow near the tube wall. Of course, the MB molecule at the back interface of the sample plug zone conversely diffuses to the high-velocity-gradient region in the center of the tube. Thus, the sample-dispersion length between the sample-zone front in the tube center and at the back in the tube wall decreases, so that the peak broadening on response-peak profiles can be minimized, as is shown in Fig. 4(b). This phenomenon can easily be understood by comparing the results obtained by using the same MB dye as a solute molecule in water and a glutinous glycerol/water (1+1) (G/W) solution as a carrier fluid, and those obtained by using the MB dye and nondiffusive submicron ink in a water carrier. When the G/W carrier was used, the measured  $d_{\text{MB}}$  value was about twice as large as the  $d_{\text{air}}$  one, because the apparent molecular diffusivity of the MB dye molecule in the G/W solution is negligibly small, probably less than  $10^{-5} \text{ mm}^2 \text{ s}^{-1}$ . The relationship between the measured  $d_{\text{MB}}$  and  $d_{\text{air}}$  values is studied in this work. The ordinate represents the slopes of the  $d_{\text{MB}}$  values in Fig. 3; the abscissa represents those of the  $d_{\text{air}}$  values. The results obtained by using glass tubes with an inner diameter between 0.5 mm and 1 mm i.d. show that a narrower glass column has a larger velocity gradient and that the profile of the colored sample plug loses its sharpness as a result of the molecular diffusivities of the solute molecules into a water carrier larger than  $10^{-4} \text{ mm}^2 \text{ s}^{-1}$ . The model apparatus is, therefore, useful for fundamental and experimental studies of the dispersion behavior of an injected sample plug containing solute molecules as tracers in a flowing carrier stream in small-bore glass tubes.

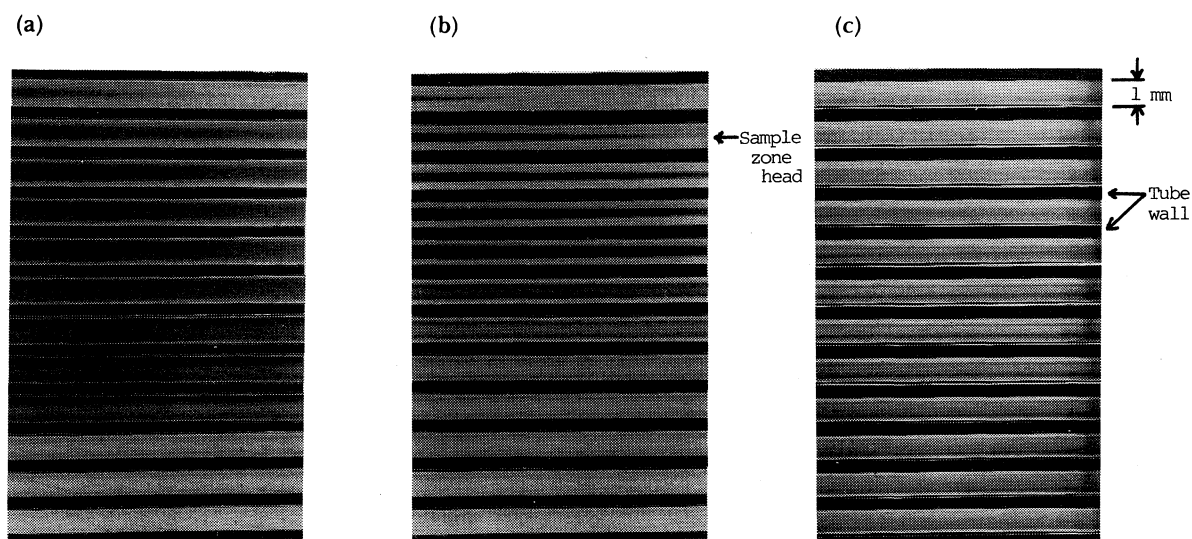


Fig. 5. Photographs continuously obtained with a microscope for the mobile sample plug zones. Ten- $\mu\text{l}$  of 1 mM MB dye or submicron particle ink solutions were injected by the open-column method into a water carrier. A glass tubing (1 mm i.d. and 200 mm detection distance) was used as a capillary column. (a) MB dye; flow velocity:  $11.9 \text{ mm s}^{-1}$ , (b) MB dye; flow velocity:  $110 \text{ mm s}^{-1}$ , and (c) submicron ink; flow velocity:  $21 \text{ mm s}^{-1}$ .

**Flow Pattern Analysis by Means of a Photographic Method with a Microscope.** A typical flow pattern, obtained by the present photographic method with a microscope, is shown in Fig. 5, where the mobile colored sample zone travels through the capillary tube. According to the procedure, a motor-drive camera starts and many photographs are continuously taken, using a 100-foot roll film, as soon as the injected sample zone front enters the view of the microscope. The photographs show that the injected-sample zone flows with the laminar-flowing carrier fluid and rapidly broadens along with the flow-velocity profile in the axial direction. The flowing sample zone contains a sharply-pointed, needle-like top and has two parabolic interfaces (front and back) lying between the sample plug and the carrier fluid. According to the parabolic-velocity distribution in the laminar flow, represented by Eq. 1, the flow pattern of the sample zone becomes sharper with the increase in the flow rate of the carrier fluid, as is shown in Figs. 5(a) and 5(b). This result is due to the difference in the diffusion time.

Many photographs were taken for the MB-dye samples under various operating conditions by changing the flow rate and the tube length. All the photographs show the same results as those presented above; that is, the sample zone became sharper and spread wider in the axial direction with an increase in the flow rate and/or the tube length. The mixing of the sample component (i.e., the solute) with the carrier component depends on the convection (i.e., the laminar flow profile), and their molecular diffusivities occurred at the parabolic interfaces (front and back). By comparing Figs. 5(a) and (b), it is also found that the interfaces become more distinct because of the smaller extension of the molecular diffusion when the flow rate becomes faster, viz., when the mean residence time ( $t_m = L/u$ ) decreases. Furthermore, when the nondiffusive ink sample was injected, the front and back interfaces were much more distinct than the diffusive ones because the molecular diffusion of the component substances was one of the most important parameters in controlling peak dispersion (cf. the

photographs in Fig. 5(c)).

**Peak-Dispersion Observation by Means of a Micro-Photometric-Detection System.** In stead of the qualitative photographic method, the hand-made micro-photometric-detection system developed here was used to evaluate quantitatively the axial dispersion, that is, the sample-zone broadening as the response-peak profile. In order to optimize the operating conditions in several analytical instrumentation methodologies using small-bore tubes as reactors, the physical properties of the injected-sample plug and the carrier solutions are the most important parameters for the design of the flowing systems. The effects of the molecular diffusivities of the solutes were first studied; the peak features are shown in Fig. 6. For a large molecular diffusivity (i.e., the potassium permanganate solute), the second peak is more apparent than the first one, the width of the peak feature being much narrower and the dispersion in the axial direction being reduced because of the molecular diffusion of the solute in the radial direction in the water carrier. When the ink sample, which contains colored sub-micron particles and has much less molecular diffusivity than the potassium permanganate and MB-dye samples, is injected as the sample plug, the double-peak features cannot be obtained as expected for a molecule having a molecular-diffusion coefficient of less than  $10^{-5} \text{ mm}^2 \text{ s}^{-1}$  by means of the computer simulation.<sup>10)</sup>

The response-peak features under various operating conditions are very interesting, as is shown in Fig. 7. Nine figures are summarized at different flow rates and different tube lengths in the present apparatus with a horizontally placed capillary tube (Fig. 2). Almost all of these response peaks show the clear double-humped peak features expected from computer simulation using the numerical-analysis method.<sup>8)</sup> This means that the experimental apparatus used in this study is quite satisfactory for studying the dispersion behavior of the solutes in a laminar capillary flow, since many theoretical analyses were carried out on the basis of the assumption that the flow was really laminar.<sup>4-8)</sup> From these figures, the sharper part (the first peak) is seem to

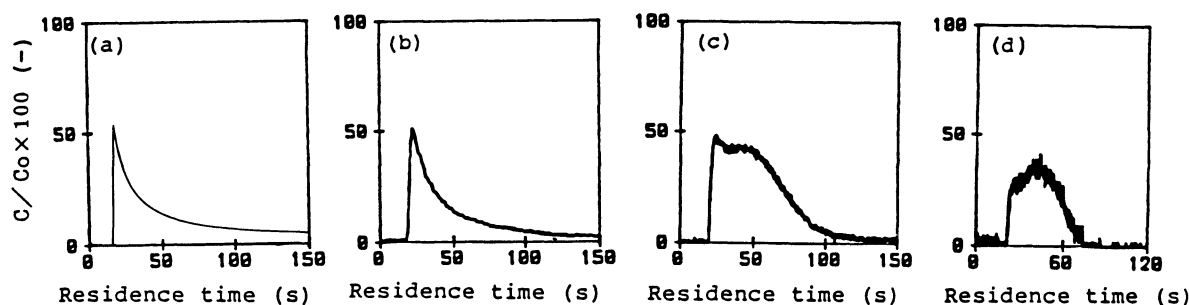


Fig. 6. Difference of peak features for different molecular diffusion coefficient samples. (a) Simulation results for nondiffusive solute, (b) submicron particle ink, (c) MB dye, and (d) potassium permanganate. Each  $10 \mu\text{l}$  of the sample solutions was injected into distilled water flowing in a 1 mm i.d. and 400 mm length glass tubing as a capillary column.

result from convection by the parabolic-velocity profiles, while the other part (the second peak) is caused by the molecular diffusion of the solute injected as the plug of the sample solution.

It may be found in Fig. 7 that the second diffusion peak becomes more apparent when the flow rate is relatively slow and that the peak height becomes lower and the peak width increases with a longer traveling distance (i.e., tube length). When the column reactor

becomes longer in various analytical instruments, the sample zone is dispersed along with a longer laminar-flow velocity profile in the axial direction; the large concentration distribution of the solute in the sample solution causes the lower peak-height response. It can also be found that the response-peak feature becomes nearly a Gaussian distribution for a long retention time (e.g., for a long traveling distance and/or a slow flow rate).

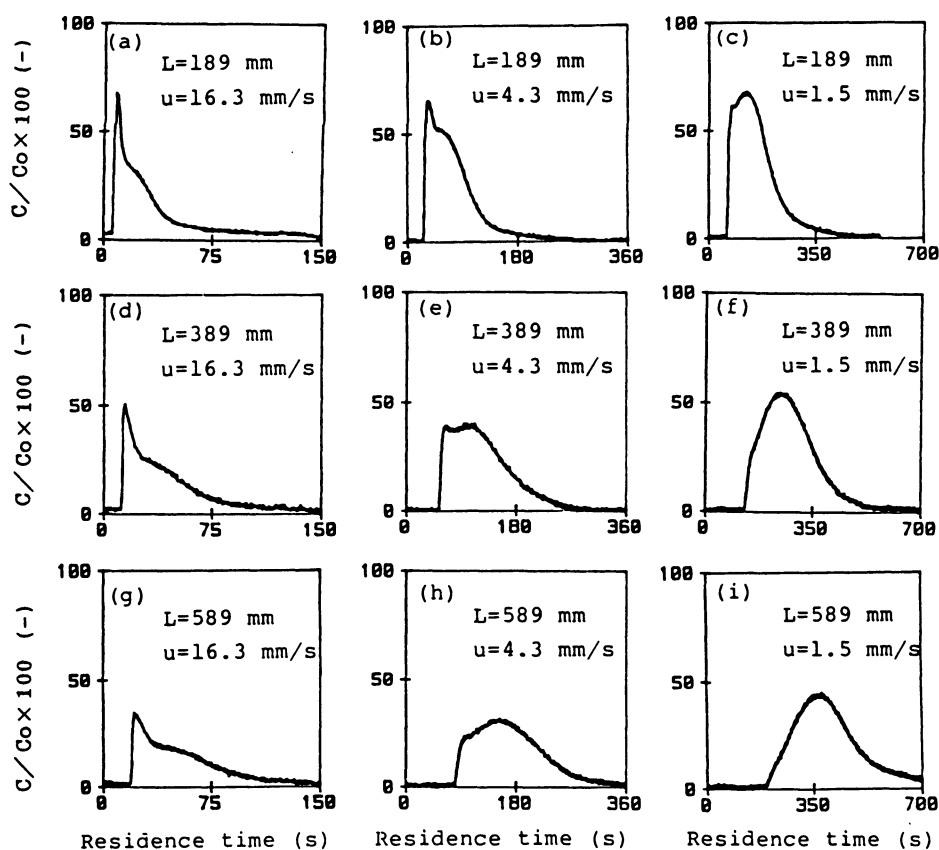


Fig. 7. Peak features obtained for MB dye sample solutions by the microphotometric detection system. Capillary column: 1 mm i.d. glass tubing. Carrier fluid: distilled water.  $u$  denotes the average velocity,  $c$  and  $c_0$  denote the respective and original concentrations of the MB dye sample respectively.

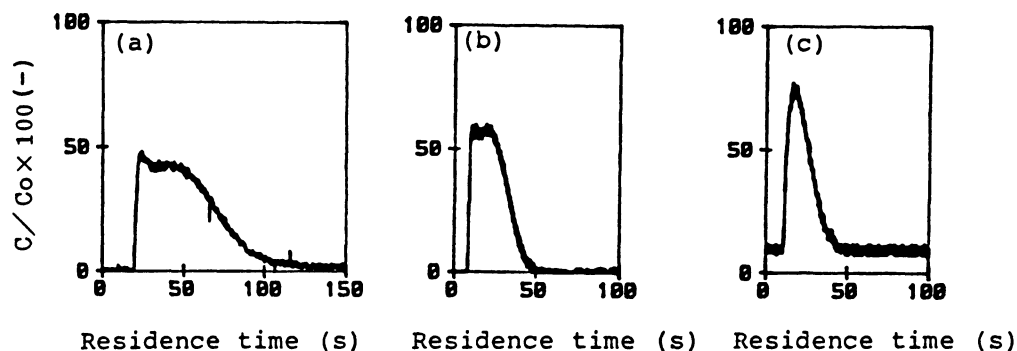


Fig. 8. Peak features obtained by changing capillary conditions. MB dye sample and a 400 mm length glass tubing were used. (a) 1 mm i.d. straight capillary column, (b) 0.6 mm i.d. straight capillary column, and (c) 0.6 mm i.d. coiled capillary column (one loop, 100 mm in loop diameter) were used.

Figs. 8(a) and (b) directly illustrate the qualitative results for the column-radius effect on the peak features. It is found that the narrower capillary tube is effective in obtaining a higher and narrower peak. When the inner diameter of the capillary column decreases, the velocity profile becomes more abrupt between the wall and the center of the capillary tube, according to Eq. 1. Thus, the sample broadening in the axial direction is strongly reduced by the molecular diffusion in the radial direction.

Peak broadening, caused by the sample dispersion in the capillary columns, may generally be far more reduced in the coiled capillary tubes than in straight tubes in consequence of the coiling effect induced by the secondary flow phenomenon,<sup>12</sup> for the secondary flow effectively enhances mixing and mass transfer in the radial direction. Coiled capillary tubes are, therefore, examined in this work. As is also shown in Figs. 8(b) and 8(c), on the basis of Tijssen's theoretical work on FIA<sup>12</sup> it has been concluded that peak broadening can be far more reduced by coiling tubes than in straight tubes in consequence of the coiling effect induced by the secondary flow phenomenon. Because the secondary flow enhances mixing and mass transfer in the radial direction, reduces the dispersion in the axial direction, its peak feature consequently becomes nearly a Gaussian distribution, as is suggested by Fig. 8(c). It is, therefore, recommended that the column of CLC also be coiled into a helical configuration in order to reduce the peak broadening and to obtain a high sensitivity and resolution.

**Traveling Distance and Sample Arrival Time.** As has been noted in the former section, the traveling distance of the sample-zone head ( $d_{\text{head}}$ ) is smaller than that calculated because of molecular diffusion. A similar phenomenon of the shortening effect can also be seen by comparing the sample traveling time

measured ( $t_a$ ) with the one calculated (Fig. 9). Figure 9 shows the relationship between the measured  $t_a$  value and the tube length. Each broken line is a theoretical line based on Eq. 3. All the  $t_a$  values measured seem to be larger than the theoretical values since the sample-zone head has lost its sharpness by molecular diffusion at the front of the interfaces, as is suggested in Fig. 4(b). Hence, it requires a longer arrival time for the sample-plug-zone head to reach the detector view.

**Effect of Flow Rate.** The variations in the peak height as a function of the flow rate are shown in Fig. 10 for different lengths of tubes. As the peak consists of double-humped peak features, the peak-height data presented here are the heights of the higher among the first- and second-peak features. The flow rate at which the peak height reaches a minimum just corresponds to the double-humped peaks with the same two peak heights, that is, a critical flow rate (CFR). At just this point, both diffusion and convection are found significant. Below this critical point on the flow rate, the second peak is higher than the first one because of sufficient molecular diffusions; thereafter, its height decreases with the increases in the flow rate, as has been discussed before. Over the point of CFR, however, the first convection peak is higher than the secondary one, because it is mainly controlled by convection. The first peak, unlike the secondary peak, represents the concentration distribution of the component substance (i.e., the solute) in the sample-plug head. The first peak height seldom varies with the flow rate, as is shown in Fig. 10, when the flow rate becomes faster. These results, therefore, show that the CFR point can be used as a judging point for the flow rate on the dispersion behavior of the response-peak features by molecular diffusion. Below the point of CFR, the peak features are controlled predominantly by the diffusion in order to make higher the peak

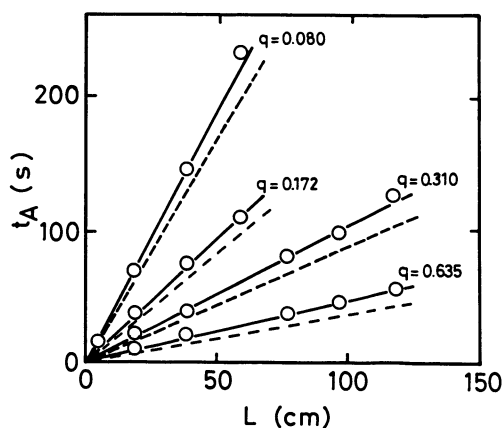


Fig. 9. Relationship between traveling time of sample zone head and the length. Each 10  $\mu$ l of MB dye sample solution was injected into distilled water flowing in a 1 mm i.d. glass capillary column.  $q$  denotes the volume flow rate, and dotted lines show the calculated values against each  $q$  values.

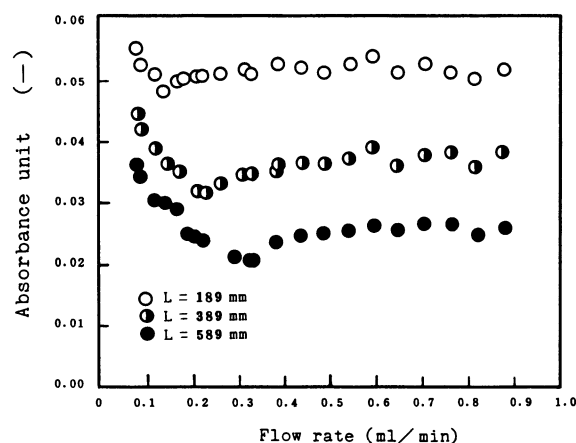


Fig. 10. Peak height value in absorbance unit vs. volume flow rate for three different tube lengths. Each 10  $\mu$ l of MB dye sample solution was injected in distilled water flowing in a 1 mm glass tubing as a capillary column.

height with the Gaussian distribution and to minimize the dispersion of the flowing-sample plug, as is shown in Fig. 10, although such slower flow-rate regions have seldom been studied.

### Discussion

The dispersion of the injected-sample plug in capillary-column reactors was experimentally investigated by means of direct observation, microscopic photographs, and photometric-detection methods newly developed. The baseline-to-baseline times are measured in those response peaks obtained by the microphotometric detection system. According to Eq. 4,<sup>10</sup> the dimensionless baseline-to-baseline time values are then compared with the dimensionless traveling-distance values (Fig. 11). It is concluded that they have a good agreement with the various experimental results obtained with the present model apparatus. This means that an ideal laminar capillary flow can be attained by the use of the model experimental apparatus described above. A great advantage of the present work is, therefore, that an ideal laminar flow can be attained by the model experimental apparatus. It is essential to use such a model apparatus for fundamental and/or experimental approaches since several theoretical analyses of this problem have been carried out on the assumption of a complete laminar capillary flow. In usual LC systems, however, disagreements between experimental and theoretical results are often found, as was pointed out first by Atwood and Golay.<sup>9</sup> They attributed the disturbance to the laminar flow resulting from the unions. Since the parts and components used in the LC, CGC, and CLC systems, such as a high-pressure double-reciprocating micropump, a loop-injection valve, or a detector with flow-through cells, cannot suppress the dead volume, abrupt changes in the internal diameter of the flowing stream, the turbulence of the flow, or the occurrence of large time constants in detectors and recorders, etc., it is not desirable to use these components for the model experiments under just a laminar flow. Before starting the work, we elaborated the apparatus in order to obtain as ideal a laminar flow as is possible. In the present experiment, a syringe pump was used to obtain a steady and smooth pumping. In order to reduce the disturbance of the laminar flow, a stopped-flow injection technique for sample injection and a hand-made microphotometric detection system were adopted. The light source and the light acceptor as the detector were mounted on the small-bore glass tube wall without any disturbance to the flowing stream. As has been described above, the results presented here show a primary success in the development of an ideally-composed model experimental apparatus for undertaking sample-dispersion-behavior analysis in capillary tubes. Although the results presented in this paper support only funda-

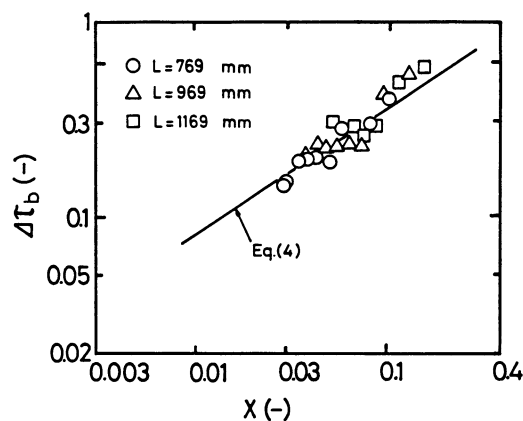


Fig. 11. Comparison of experimental results and numerical-analysis equation between dimensionless baseline-to-baseline time ( $\Delta\tau_b$ ) and dimensionless traveling distance ( $X$ ).<sup>8</sup>

mental and qualitative conclusions, they are very important to attempts to improve, design, and optimize the FIA, CLC, and other LC families.

Since the disturbance to the laminar flow by the apparatus itself has been eliminated in this work, the influences on sample dispersion by a variety of parameters, such as tube length, diameter, flow rate, and molecular-diffusion coefficient, can be clearly found, as has been discussed above. For example, Fig. 10 shows the influence of the flow rates on the peak height. For three tube lengths, below a flow rate of about 0.1 ml min<sup>-1</sup>, the peak height depends closely on the flow rate, while above that flow rate the peak height tends to be constant. Therefore, if one wants to obtain a high sensitivity by adjusting the flow rate, the operation should be conducted at flow rates below 0.1 ml min<sup>-1</sup>.

This research was funded in part by the Grants-in-Aid for Scientific Research from the Japanese Ministry of Education, Science and Culture, and also by the Shorai Foundation for Science and Technology.

### References

- 1) M. J. E. Golay, "Gas Chromatography, 1957" (Lansing Symposium), ed by V. J. Coates, H. J. Noebels, and I. S. Fagerson, Academic Press, New York (1958), p. 1.
- 2) T. Korenaga, Doctoral Dissertation, Kyoto University (1985).
- 3) L. C. Truesdell, Jr., and R. J. Adler, *Am. Inst. Chem. Eng. J.*, **16**, 1010 (1970).
- 4) G. Taylor, *Proc. R. Soc. London, Ser. A*, **219**, 186 (1953).
- 5) R. Aris, *Proc. R. Soc. London, Ser. A*, **252**, 538 (1959).
- 6) V. Ananthakrishnan, W. N. Gill, and A. J. Barduhn, *AIChE J.*, **11**, 1063 (1965).
- 7) H. Bate, S. Rowlands, J. A. Sirs, and H. W. Thomas, *Brit. J. Appl. Phys. (J. Phys. D.)*, **2**, 1147 (1969).
- 8) J. T. Vanderslice, K. K. Stewart, A. G. Rosenfeld, and D. J. Higgs, *Talanta*, **28**, 11 (1981).



- 9) J. G. Atwood and M. J. E. Golay, *J. Chromatogr.*, **218**, 97 (1981).  
10) T. Korenaga, H. Yoshida, Y. Yokota, S. Kaseno, and T. Takahashi, *J. Flow Injection Anal.*, **3**, 91 (1986).  
11) "Bussei Josu," ed by The Society of Chemical Engineers, Japan, Maruzen, Tokyo (1968), Vol. 6, p. 246.  
12) R. Tijssen, *Anal. Chim. Acta*, **114**, 71 (1980).
-